Different Regions of the HPV E7 and Ad E1A Viral Oncoproteins Bind Competitively but Through Distinct Mechanisms to the CH1 Transactivation Domain of p300.

ARTICLE *in* BIOCHEMISTRY · NOVEMBER 2012

Impact Factor: 3.02 · DOI: 10.1021/bi3011863 · Source: PubMed

BIOCHEMISTRY
including biophysical chemistry & molecular biology

Article

pubs.acs.org/biochemistry

Different Regions of the HPV-E7 and Ad-E1A Viral Oncoproteins Bind Competitively but through Distinct Mechanisms to the CH1 Transactivation Domain of p300

Daniela Fera and Ronen Marmorstein*

Program in Gene Expression and Regulation, The Wistar Institute, Philadelphia, Pennsylvania 19104, United States, and Department of Chemistry, University of Pennsylvania, Philadelphia, Pennsylvania 19104, United States

Supporting Information

ABSTRACT: p300 is a transcriptional coactivator that participates in many important processes in the cell, including proliferation, differentiation, and apoptosis. The viral oncoproteins, adenovirus (Ad) E1A and human papillomavirus (HPV) E7, have been implicated in binding to p300. The Ad-E1A–p300 interaction has been shown to result in the induction of cellular proliferation, epigenetic reprogramming, and cellular transformation and cancer. The HPV-E7–p300 interaction, on the other hand, is not well understood. p300 contains three zinc-binding domains, CH1–CH3, and studies have shown that Ad-E1A can bind to the p300 CH1 and CH3 domains whereas E7 can bind to the CH1 domain and to a lesser extent to the CH2 and CH3 domains. Here we address how high-risk HPV16-E7 and Ad5-E1A, which have different structures, can both bind the p300 CH1 domain. Using pull-down, gel filtration, and analytical ultracentrifugation studies, we show that the N-terminus and CR1 domains of Ad5-E1A and the CR1 and CR2 domains of HPV16-E7 bind to the p300 CH1 domain competitively and with midnanomolar and low micromolar dissociation constants, respectively. We also show that Ad5-E1A can form a ternary complex with the p300 CH1 domain and the retinoblastoma pRb transcriptional repressor, whereas HPV16-E7 cannot. These studies suggest that the HPV16-E7 and Ad5-E1A viral oncoproteins bind to the same p300 CH1 domain to disrupt p300 function by distinct mechanisms.

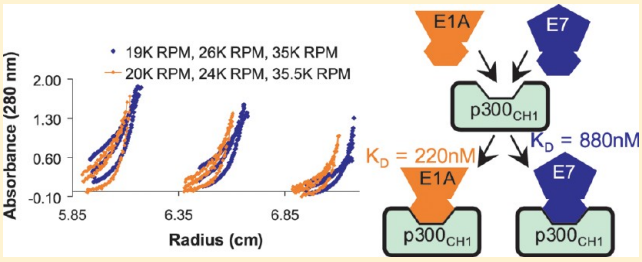

p300 is a versatile transcriptional coactivator that participates in many important processes in the cell, including proliferation, differentiation, and apoptosis.[1−3] It promotes gene transcription by acting as a protein bridge, or scaffold, that connects different transcription factors to the basic transcriptional apparatus.[3,4] This allows for the assembly of multicomponent transcription coactivator complexes.[5,6] It also has histone acetyltransferase (HAT) activity that allows it to influence chromatin structure by modulating nucleosomal histones.[7] It has also been shown to acetylate tumor suppressor transcription factors, such as p53 and pRb, thereby regulating protein function.[8,9] Therefore, p300 is involved in multiple, signal-dependent transcription events, and its deregulation is implicated in many types of diseases.[1,10,11]

Interestingly, p300 was originally identified through its specific interaction with E1A from adenovirus.[12] Ad-E1A has been shown to hijack the cellular transcription machinery by competing with essential transcription factors for binding to p300 as well as its paralog, CREB-binding protein (CBP), thereby inactivating a number of cellular and viral promoters and enhancers.[13,14] The Ad-E1A–p300 complex has been shown to stimulate cellular proliferation, whereas mutants of E1A that cannot bind p300 are defective in cellular transformation.[15] Some of these effects are also mediated by the ability of Ad-E1A to interact with the retinoblastoma protein, pRb.[16,17] Ad-E1A–p300 interactions have also been implicated in epigenetic reprogramming, leading to cellular transformation.[14] The formation of viral oncoprotein complexes with p300 has also been indicated to cause a loss of cell growth control and a block of cellular differentiation, leading to cancers.[15] The E7 protein from high-risk human papillomavirus 16 (HPV16), which is functionally homologous to Ad-E1A, but structurally dissimilar, has also been shown to bind to p300.[18] However, the downstream implications of this interaction are not well understood. HPV16-E6, the other viral oncoprotein from this virus, has also been shown to bind to and inhibit the functions of the p300–CBP complex and inhibit p53-dependent transcription.[19,20] Furthermore, this has been observed only for high-risk E6 proteins that are associated with cancerous lesions.

The viral oncoproteins E1A and E7 have been reported to bind to the transactivation zinc-finger (TAZ) domains of p300.[13,18] p300 contains two TAZ domains, called TAZ1 and TAZ2, that contain two cysteine/histidine-rich regions, called CH1 and CH3, respectively and whose primary function is protein recognition.[5] Currently, more than 30 transcription

Received: September 1, 2012
Revised: November 2, 2012
Published: November 2, 2012

factors have been found to bind to the TAZ domains.[21] The sequences of the CH1 and CH3 domains are structurally homologous but bind different proteins.[21,22] Interestingly, HPV16-E7 has been suggested to bind most prominently to the CH1 domain and to a lesser extent to the CH2 (another putative p300 zinc-finger domain) and CH3 domains, whereas Ad5-E1A was suggested to bind to the CH1 and CH3 domains of p300.[13,18,23] The interaction between Ad5-E1A and the CH1 domain, however, is not well understood. Because these viral oncoproteins bind to regions of p300 that are known to bind many transcription factors, these interactions with E7 or E1A can have many negative downstream effects in the cell.

Even though HPV16-E7 and Ad5-E1A are functionally homologous, their sequences and structures differ greatly. Both of these viral oncoproteins contain highly conserved regions CR1−CR3; however, Ad-E1A shares limited sequence homology with HPV-E7, mainly found within the strictly conserved LxCxE motif of their CR2 domains.[24,25] This motif has been shown to mediate high-affinity binding to pRb and the related pocket proteins p107 and p130.[26] The CR1 domains of these oncoproteins have some sequence similaritiy; however, the sequences of long stretches of amino acids flanking the CR1 domain of Ad-E1A are not homologous to those of HPV-E7. Interestingly, the CR1 domains appear to have different binding partners: whereas the CR1 domain of Ad-E1A can mediate binding to pRb, HPV-E7 cannot.[27] The CR3 domains are zinc-binding domains; however, Ad-E1A is a monomer, while HPV-E7 forms an obligate zinc homodimer.[28,29]

Because HPV16-E7 and Ad5-E1A are functionally homologous and structurally diverse, we were interested in biochemically comparing their binding to the p300 CH1 domain. To do this, we mapped the domains of the viral oncoproteins that were required for $p300_{CH1}$ binding and quantified their interactions using analytical ultracentrifugation sedimentation equilibrium studies. The dissociation constants of the Ad5-E1A−$p300_{CH1}$ and HPV16-E7−$p300_{CH1}$ complexes were found to be in the midnanomolar and low micromolar range, respectively, indicative of strong interactions. Furthermore, we were able to show that these viral oncoproteins bind competitively to $p300_{CH1}$, suggesting that they may bind to the same site on $p300_{CH1}$. We also show that Ad5-E1A can form a ternary complex with the p300 CH1 domain and the retinoblastoma pRb transcriptional repressor, whereas HPV16-E7 cannot. These studies suggest that the HPV16-E7 and Ad5-E1A viral oncoproteins may bind to a common surface on $p300_{CH1}$ to disrupt p300 function by distinct mechanisms.

EXPERIMENTAL PROCEDURES

Expression and Purification of Proteins. *GST-Tagged E7 and E1A Proteins.* The DNA encoding Ad5-$E1A_{1-77}$, Ad5-$E1A_{1-138}$, HPV16-$E7_{1-98}$ (full length), HPV16-$E7_{17-98}$, HPV16-$E7_{46-98}$, HPV16-$E7_{1-51}$, HPV16-$E7_{1-46}$, HPV16-$E7_{17-46}$, HPV16-$E7_{1-17}$, and HPV1A-$E7_{1-93}$ (full length) were cloned into the pGEX-4T-1 vector, containing an N-terminal GST tag. Proteins were expressed in *Escherichia coli* BL21(DE3) cells overnight at 18 °C using 1 mM IPTG; 100 μM $Zn(OAc)_2$ was also added at induction to constructs containing a zinc-binding domain (HPV16-$E7_{1-98}$, HPV16-$E7_{17-98}$, HPV16-$E7_{46-98}$, and HPV1A-$E7_{1-93}$). Cells were lysed by sonication in a buffer containing 1× PBS (pH 7.4), 100 mM NaCl, 10 mM BME, and 1× PMSF; 10 μM $Zn(OAc)_2$ was added to the lysis buffer of constructs containing a zinc-binding domain. The cell lysate was centrifuged at 18000 rpm for 30 min, and the resulting supernatant was loaded onto GST superflow resin (Clontech) pre-equilibrated with 1× PBS (pH 7.4), 100 mM NaCl, and 10 mM BME. The column with protein loaded was then washed with the same buffer. The GST-fused protein was then eluted using 1× PBS (pH 7.4), 100 mM NaCl, 10 mM GSH, and 10 mM BME. The eluent was then concentrated and further purified using a Superdex analytical column (GE Healthcare Life Sciences) in a buffer containing 20 mM Tris (pH 7.5), 150 mM NaCl, and 10 mM BME.

Untagged HPV-E7 Proteins. To purify untagged HPV-E7 constructs, HPV-E7 was expressed and purified as a GST fusion as described above. After the GST superflow column had been loaded and the contaminants washed off, the protein was subjected to thrombin (Enzyme Research) cleavage at 20 °C for 1 h. The cleaved protein and protease were washed off the column. Ion exchange was then performed to separate E7 from the thrombin using a high-trap Q HP column (Fisher) with a salt gradient {buffer A [20 mM Tris (pH 7.5), 50 mM NaCl, and 10 mM BME] and buffer B [20 mM Tris (pH 7.5), 750 mM NaCl, and 10 mM BME]}. Fractions containing HPV-E7 were pooled, concentrated, and run via gel filtration using a Superdex 200 analytical column (GE Healthcare Life Sciences) in a buffer containing 20 mM Tris (pH 7.5), 150 mM NaCl, and 10 mM BME.

His-Tagged Ad5-E1A and HPV16-E7 Proteins. The DNA for Ad5-$E1A_{1-189}$, Ad5-$E1A_{77-189}$, Ad5-$E1A_{138-189}$, Ad5-$E1A_{1-138}$, and Ad5-$E1A_{1-77}$ was cloned into a pET vector containing an N-terminal six-histidine tag. HPV16-$E7_{1-98}$ was cloned into the pRSET vector, also containing an N-terminal six-histidine tag. Ad5-E1A and HPV16-E7 were expressed in *E. coli* BL21(DE3) cells overnight at 18 and 25 °C, respectively, using 1 mM IPTG; 100 μM $Zn(OAc)_2$ was also added at induction to constructs containing a zinc-binding domain (Ad5-$E1A_{1-189}$, Ad5-$E1A_{77-189}$, Ad5-$E1A_{138-189}$, and HPV16-$E7_{1-98}$). Cells were lysed by sonication in a buffer containing 20 mM Tris (pH 7.5), 500 mM NaCl, 35 mM imidazole, 10 mM BME, and 1× PMSF; 10 μM $Zn(OAc)_2$ was added to the constructs containing the zinc-binding domain. The cell lysate was centrifuged at 18000 rpm for 30 min, and the resulting supernatant was loaded onto a Ni-NTA column (Fisher) pre-equilibrated with 20 mM Tris (pH 7.5), 500 mM NaCl, 35 mM imidazole, and 10 mM BME. The column was washed, and the bound protein was eluted using an imidazole gradient from 35 to 250 mM. Ion exchange was then performed using a high-trap Q HP column (Fisher) with a salt gradient {buffer A [20 mM Tris (pH 7.5), 50 mM NaCl, and 10 mM BME] and buffer B [20 mM Tris (pH 7.5), 750 mM NaCl, and 10 mM BME]}. Fractions containing the desired protein were pooled, concentrated, and run via gel filtration using a Superdex 200 analytical column (GE Healthcare Life Sciences) in a buffer containing 20 mM Tris (pH 7.5), 150 mM NaCl, and 10 mM BME.

p300. The DNA encoding the CH1 domain of human p300 (residues 323−424) was cloned into the pGEX-4T-1 vector, containing an N-terminal GST tag. The protein was expressed, lysed, and purified, as described above for the GST-tagged HPV-E7 proteins with a zinc-binding domain. To generate untagged p300, the protein was subjected to on-column cleavage with TEV. The protease was removed by binding to Ni-NTA resin (Fisher). Ion exchange was then performed using a high-trap SP HP column (Fisher) with a salt gradient {buffer A [20 mM Tris (pH 7.5), 50 mM NaCl, and 10 mM BME] and buffer B [20 mM Tris (pH 7.5), 750 mM NaCl, and 10 mM

dx.doi.org/10.1021/bi3011863 | *Biochemistry* 2012, 51, 9524−9534

BME]}. Fractions containing the desired protein were pooled, concentrated, and run via gel filtration using a Superdex 200 analytical column (GE Healthcare Life Sciences) in a buffer containing 20 mM Tris (pH 7.5), 150 mM NaCl, and 10 mM BME.

GST Alone. To make GST protein as a control for pull-down experiments, we transformed the pGEX-4T-1 vector into BL21(DE3) cells and expressed and purified it the same way as the GST-fused proteins.

pRb. Domains A and B of pRb used in pull-down experiments were expressed and purified as described previously.[30]

Pull Downs. Thirty micrograms of GST protein (final concentration of 1−4 μM) was incubated with 25 μL of GST superflow resin (Clontech) that was prewashed in binding buffer for 15 min at 4 °C, and an equimolar amount of the binding partner to be tested was added to the mixture with incubation for 1 h with gentle rotation at 4 °C. For formation of the ternary complex, an additional 1 h incubation was used for the third protein. The buffer used in each pull down is given in the text and determined on the basis of the ability to form a complex and the ability of the proteins to stay in solution. The final reaction volume was approximately 300−400 μL. The beads were then collected by centrifugation at 600*g* and 4 °C for 5 min and washed three times using 1 mL of binding buffer. Samples were then subjected to sodium dodecyl sulfate−polyacrylamide gel electrophoresis (SDS−PAGE) analysis. For competition experiments, 12.5 μg of GST protein was incubated with 10 μL of GST superflow resin (Clontech) in a buffer consisting of 20 mM Tris (pH 8.0), 100 mM NaCl, 10 mM BME, and 0.05% Tween 20. The binding partner was then incubated with the GST-tagged protein for 1 h prior to the addition of different concentrations of competitor protein. After another incubation for 1 h, the beads were washed as described above, run on an SDS−PAGE gel, transferred to PVDF membrane, and then probed with anti-His (1:5000, Fisher), anti-HPV16-E7 (1:5000, Abcam), and anti-GST (1:5000, Millipore) antibodies, followed by an anti-mouse antibody conjugated to HRP (1:5000, Bio-Rad). Bands were visualized by chemiluminescence (Pierce) and exposed to film (Kodak).

Size Exclusion Chromatography. To determine if the viral oncoproteins coelute with $p300_{CH1}$, equimolar amounts of each protein were added to a final volume of approximately 1 mL of buffer (as indicated in the text). The proteins were incubated for at least 1 h prior to running on either a pre-equilibrated Superdex 200 analytical column (Fisher Scientific) for the samples with Ad-E1A proteins or a pre-equilibrated Superdex 75 preparatory column (Amersham Biosciences) for the samples with HPV-E7 proteins.

Equilibrium Sedimentation. Analytical ultracentrifugation of the Ad5-E1A−p300 and HPV16-E7−p300 complexes, as well as individual proteins, were performed at 4 °C with absorbance optics using a Beckman Optima XL-I analytical ultracentrifuge, using a four-hole rotor. The partial specific volume and viscosity were estimated by using Sednterp.[31] Analysis was performed by using six-channel centerpieces with quartz windows. To ensure equilibrium was reached, scans were performed every 4 h and compared. Protein samples were analyzed at three different protein and protein complex concentrations; optical densities of 0.3, 0.5, and 0.7 were used. A global fit of the data was performed for each sample using HeteroAnalysis. The quality of fit was assessed from the root-mean-square deviation (rmsd).

RESULTS

$p300_{CH1}$ Binds Strongly to Ad5-E1A, HPV16-E7, and HPV1A-E7 but with Differing Affinities. Ad5-E1A and HPV-E7 have been implicated to interact with the CH1 domain of p300;[1,18,23] therefore, we wanted to compare the binding of these different viral oncoproteins to $p300_{CH1}$. We first wanted to determine whether full-length high-risk HPV16-$E7_{1-98}$ or low-risk HPV1A-$E7_{1-93}$ proteins bind to $p300_{CH1}$ and if so whether they bind with similar or differing affinities. To test this, full-length E7 protein from each form of HPV was expressed with an N-terminal GST tag and tested at a final concentration of 2.6 μM. Binding was assessed with in vitro pull-down assays on GST beads with equimolar amounts of untagged $p300_{CH1}$. The buffer used for these studies consisted of 20 mM Tris (pH 8.0), 100 mM NaCl, 10 mM BME, and 0.05% Tween 20, and the samples were analyzed by SDS−PAGE. As can be seen in Figure 1A, a very faint band is observed in the HPV1A-E7 lane with a darker band in the HPV16-E7 lane, suggesting that high-risk HPV16-E7 binds more strongly than low-risk HPV1A-E7 to $p300_{CH1}$. $p300_{CH1}$ did not bind to GST alone, indicating that the binding to E7 was specific and not mediated by $p300_{CH1}$ nonspecific aggregation.

Because high-risk HPV16-E7 bound to $p300_{CH1}$ with a greater apparent affinity than low- risk HPV1A-E7, we next wanted to compare the binding of full-length HPV16-E7 and the CR1−CR3 domains of Ad5-E1A to $p300_{CH1}$. For these studies, $p300_{CH1}$ was fused to a GST tag and HPV16-$E7_{1-98}$ and Ad5-$E1A_{1-189}$ were expressed with N-terminal six-histidine tags. Similarly, pull-down assays were conducted with GST beads with viral oncoproteins and the GST-$p300_{CH1}$ fusion protein at protein concentrations of 2.6 and 3.7 μM, respectively, with the same buffer described above, and binding was assessed by running the samples on an SDS−PAGE gel. As can be seen in Figure 1B, the retained band for 6×His-Ad5-$E1A_{1-189}$ was much darker than the corresponding band for 6×His-HPV16-$E7_{1-98}$, suggesting that Ad5-$E1A_{1-189}$ binds more tightly to $p300_{CH1}$ than HPV16-$E7_{1-98}$. 6×His-Ad5-$E1A_{1-189}$ and 6×His-HPV16-$E7_{1-98}$ did not bind to the control GST only sample, indicating that the interactions of $p300_{CH1}$ with Ad5-$E1A_{1-189}$ and HPV16-$E7_{1-98}$ were specific and that they were not forming aggregates.

The CR1 Domain of Ad5-E1A Is Necessary for Interaction with $p300_{CH1}$. Because Ad5-$E1A_{1-189}$ was able to bind to $p300_{CH1}$, we next wanted to map the site of interaction on Ad5-$E1A_{1-189}$. To do this, different deletion constructs of 6×His-Ad5-$E1A_{1-189}$ were made [6×His-Ad5-$E1A_{1-138}$, 6×His-Ad5-$E1A_{1-77}$, 6×His-Ad5-$E1A_{77-189}$, and 6×His-Ad5-$E1A_{138-189}$ (Figure 2A)] and tested for their ability to bind to the GST-$p300_{CH1}$ fusion protein at protein concentrations of 2.6 μM using pull downs in a buffer consisting of 20 mM Tris (pH 8.0), 100 mM NaCl, 10 mM BME, and 0.05% Tween 20. As can be seen in Figure 2B, 6×His-Ad5-$E1A_{1-189}$ and 6×His-Ad5-$E1A_{1-138}$ appeared to bind with similar affinities, suggesting that the CR3 domain of Ad5-E1A is not necessary for binding to $p300_{CH1}$. This was further confirmed by the fact that 6×His-Ad5-$E1A_{138-189}$ (containing regions C-terminal to the CR2 domain) did not show detectable binding to $p300_{CH1}$ (Figure 2C). 6×His-Ad5-$E1A_{1-77}$ (containing the N-terminus and CR1 domain) also showed significant binding, although the level of binding appeared to be reduced (Figure 2B). To determine if residues

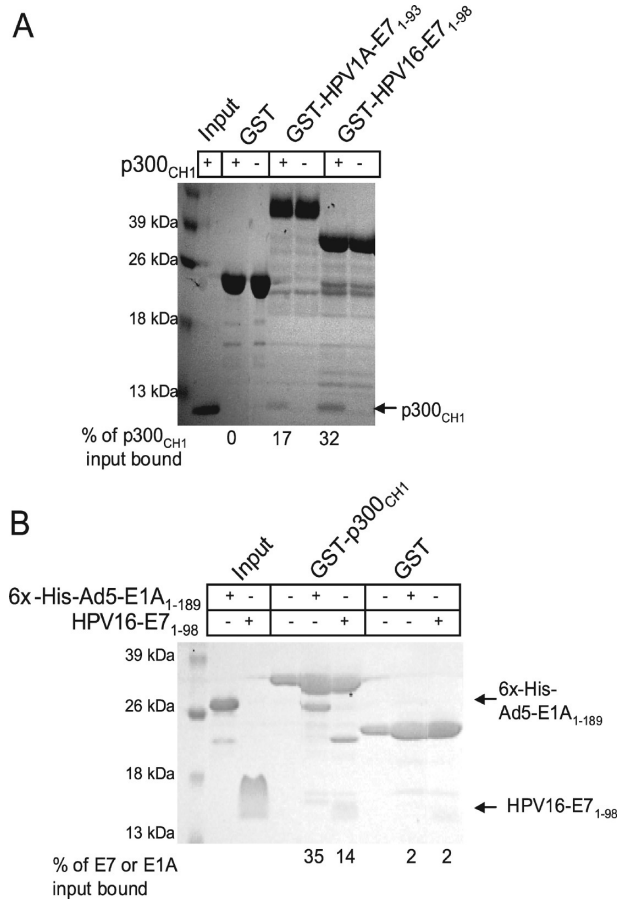

Figure 1. Pull downs between p300 and the viral oncoproteins. (A) Comparison of the binding of HPV1A-E7 and HPV16-E7 to the CH1 domain of p300. An SDS−PAGE gel is shown for pull downs done between equimolar amounts of $p300_{CH1}$ and GST-tagged full-length HPV-E7 proteins each tested at a final concentration of 2.6 μM; 3.7 μM GST was used as a control to ensure that $p300_{CH1}$ does not bind to the tag. (B) Comparison of the binding of 6×His-Ad5-E1A and untagged HPV16-E7 to $p300_{CH1}$. An SDS−PAGE gel is shown for pull downs done between GST-tagged $p300_{CH1}$ and untagged HPV16-E7 or 6×His-Ad5-E1A each tested at a final concentration of 2.6 μM. Thrombin that has not been completely removed from the HPV16-E7 purification cleaved a small amount of the GST-$p300_{CH1}$ protein, resulting in an additional band, shown in lane 6. GST (3.7 μM) was used as a control to ensure that HPV16-E7 and Ad5-E1A do not bind to the tag.

77−138 were important for $p300_{CH1}$ binding, 6×His-Ad5-$E1A_{77-189}$ was tested and shown not to interact with $p300_{CH1}$, suggesting that Ad5-$E1A_{1-77}$ is necessary and possibly sufficient for interaction with $p300_{CH1}$ (Figure 2C).

Because an interaction could be seen between Ad5-E1A and $p300_{CH1}$ using pull-down experiments, we next wanted to determine if stable complexes of these two proteins could be isolated for more quantitative analysis. To test this, the different constructs of 6×His-Ad5-E1A that bind to $p300_{CH1}$ were mixed at a concentration of approximately 40−80 μM with the same concentration of $p300_{CH1}$ and incubated for 1 h before the complex was run on a Superdex 200 analytical column in a buffer consisting of 20 mM Tris (pH 8.0), 100 mM NaCl, and 5 mM BME. Because 6×His-Ad5-$E1A_{1-77}$ had many impurities, an untagged construct was made by expressing it as a GST fusion. Consistent with results from the pull-down experiments, 6×His-Ad5-$E1A_{1-189}$, 6×His-Ad5-$E1A_{1-138}$, and untagged Ad5-$E1A_{1-77}$ were able to coelute with $p300_{CH1}$, as indicated by SDS−PAGE gels and by the shift in the gel filtration peak when compared to those of $p300_{CH1}$ alone (Figure 2D). These results suggested that Ad5-E1A constructs containing residues 1−77 could form stable complexes with $p300_{CH1}$.

The CR1 and CR2 Domains of HPV16-E7 Are Necessary for the Interaction with $p300_{CH1}$. Because E1A and E7 are functionally homologous and we were able to demonstrate that residues 1−77 of Ad5-E1A, corresponding to its N-terminus and CR1 domain, are necessary for binding to $p300_{CH1}$, we wanted to determine which domains of HPV16-E7 are needed for complex formation. This was especially of interest because the sequence of the N-terminus of Ad5-E1A is not at all homologous to that of HPV16-E7. To map regions of HPV16-E7 that were required for $p300_{CH1}$ interaction, we prepared different deletion constructs of GST-tagged HPV16-E7 [GST-HPV16-$E7_{17-98}$, GST-HPV16-$E7_{46-98}$, GST-HPV16-$E7_{1-51}$, GST-HPV16-$E7_{1-46}$, GST-HPV16-$E7_{17-46}$, GST-HPV16-$E7_{1-17}$, and GST-HPV16-$E7_{1-98}$ (full length) (Figure 3A)] to compare their abilities to bind to $p300_{CH1}$ using pull downs in a buffer consisting of 20 mM Tris (pH 8.0), 50 mM NaCl, 10 mM BME, and 0.05% Tween 20 (Figure 3B). Proteins were tested at a final concentration of 3 μM. As can be seen in Figure 3B, all of the constructs were able to bind to $p300_{CH1}$ except for the GST-HPV16-$E7_{46-98}$ construct (containing only the CR3 domain). Of note, HPV16-$E7_{1-98}$, HPV16-$E7_{1-51}$, and HPV16-$E7_{1-46}$ bound to $p300_{CH1}$ most strongly, HPV16-$E7_{17-98}$ bound more weakly, and HPV16-$E7_{1-17}$ and HPV16-$E7_{17-46}$ bound the weakest. These results suggest that the CR2 domain, consisting of residues 17−46, was necessary but not sufficient for the interaction with $p300_{CH1}$. In fact, both the CR1 and CR2 domains of HPV16-E7, consisting of residues 1−46, appeared to be sufficient for $p300_{CH1}$ interaction. As was the case for Ad5-E1A, the CR3 domain of HPV16-E7 (residues 46−98) did not appear to interact at all with $p300_{CH1}$ (Figure 3B).

Because interactions could be seen between HPV16-E7 and $p300_{CH1}$ using pull-down experiments, complexes formed between the different HPV16-E7 constructs and $p300_{CH1}$ were run on a Superdex 75 preparatory column to assess if stable complexes could form. Untagged HPV16-E7 constructs, at a concentration of approximately 100−140 μM, were used for these experiments, and they were combined with $p300_{CH1}$ at the same final concentration. Size exclusion chromatography was conducted with a buffer of 20 mM Tris, 50 mM NaCl, and 10 mM BME. The buffer was adjusted to pH 8.0 for HPV16-$E7_{1-98}$ and HPV16-$E7_{17-98}$ and to pH 7.0 for HPV16-$E7_{1-51}$. These proteins were also run individually for comparison against any complexes that formed. Consistent with results from the pull-down experiments, only HPV16-$E7_{1-98}$ and HPV16-$E7_{1-51}$ revealed coelution with $p300_{CH1}$, suggesting that a stable complex was formed between the two proteins (Figure 3C,D). Interestingly, HPV16-$E7_{1-98}$ and HPV16-$E7_{1-51}$ did not coelute with $p300_{CH1}$ when using a buffer with a higher salt concentration (20 mM Tris, 100 mM NaCl, and 10 mM BME), suggesting that E7 binds with a lower affinity to p300 than E1A, consistent with our previous results (Figure 1B). HPV16-$E7_{17-98}$, for which the binding to $p300_{CH1}$ was weaker, did not coelute with $p300_{CH1}$ (data not shown). As indicated from the SDS−PAGE gels, adding HPV16-E7 to $p300_{CH1}$ shifted the elution pattern to the left, when compared to that of $p300_{CH1}$ alone, indicative of complex formation (Figure 3C,D).

dx.doi.org/10.1021/bi3011863 | *Biochemistry* 2012, 51, 9524−9534

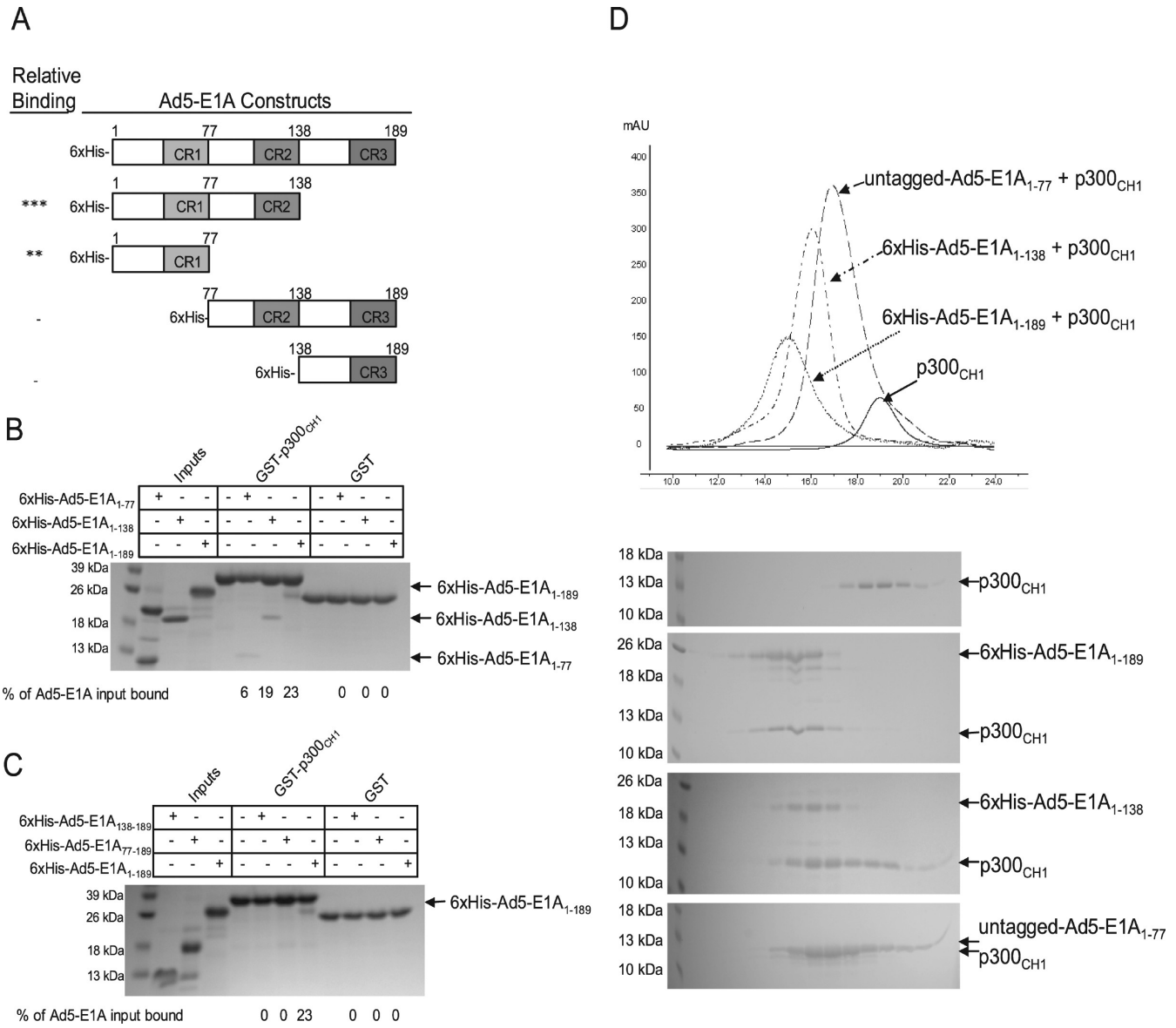

Figure 2. Mapping the interaction between Ad5-E1A and $p300_{CH1}$. (A) Constructs of 6×His-Ad5-E1A that were tested in pull-down experiments. The asterisks in the left column indicate the level of binding as compared to that of 6×His-Ad5-$E1A_{1-189}$, with more asterisks suggesting a stronger interaction with $p300_{CH1}$. A minus sign indicates that no interaction was observed. (B) Pull downs with C-terminal deletions of 6×His-Ad5-E1A. An SDS−PAGE gel is shown for each pull down done between $p300_{CH1}$ and the different constructs of Ad5-E1A each tested at a final concentration of 2.6 μM. The stronger upper band in the input lane for $E1A_{1-77}$ in panel B is a contaminant that was obtained from the expression of this construct in *E. coli* that could not be separated during the purification process. (C) Pull downs with N-terminal deletions of 6×His-Ad5-E1A. An SDS−PAGE gel is shown for each pull-down experiment done between $p300_{CH1}$ and the different constructs of 6×His-Ad5-E1A each tested at a final concentration of 2.6 μM. (D) Gel filtration between 6×His-Ad5-E1A or untagged Ad5-E1A and $p300_{CH1}$. The chromatograms from size exclusion chromatography for the different complexes (final protein concentrations tested ranging from 40 to 80 μM), as well as for $p300_{CH1}$ alone, are shown with the elution profiles using SDS−PAGE gels. The peaks in the gels are aligned with the corresponding peaks in the chromatograms.

HPV16-E7 and Ad5-E1A Bind Competitively to $p300_{CH1}$. Our data indicate that the N-terminus and CR1 domain of Ad5-E1A and the CR1 and CR2 domains of HPV16-E7 are necessary and sufficient for interaction with $p300_{CH1}$. These regions of the viral oncoproteins have very limited sequence homology, suggesting that they might bind to different regions of $p300_{CH1}$. To test this, pull downs were performed in which either 1 μM 6×His-Ad5$E1A_{1-77}$ or untagged $HPV16\text{-}E7_{1-98}$ was preincubated with GST-tagged $p300_{CH1}$ on GST beads and then titrated with different concentrations of either untagged $HPV16\text{-}E7_{1-98}$ or 6×His-Ad5$E1A_{1-77}$, respectively, in a buffer consisting of 20 mM Tris (pH 8.0), 100 mM NaCl, 10 mM BME, and 0.05% Tween 20. The amount of viral oncoprotein remaining bound was determined by Western blotting. Surprisingly, as shown in panels A and B of Figure 4, each viral oncoprotein was able to compete with the other for binding to $p300_{CH1}$. This suggests that these two viral oncoproteins bind competitively to $p300_{CH1}$ and possibly bind to the same region of the CH1 domain of p300.

$p300_{CH1}$ Binds with a 1:1 Stochiometry to the Viral Oncoproteins. Because stable complexes could be formed between the viral oncoproteins and $p300_{CH1}$, their binding stoichiometry and dissociation constants were determined. To

dx.doi.org/10.1021/bi3011863 | *Biochemistry* 2012, 51, 9524−9534

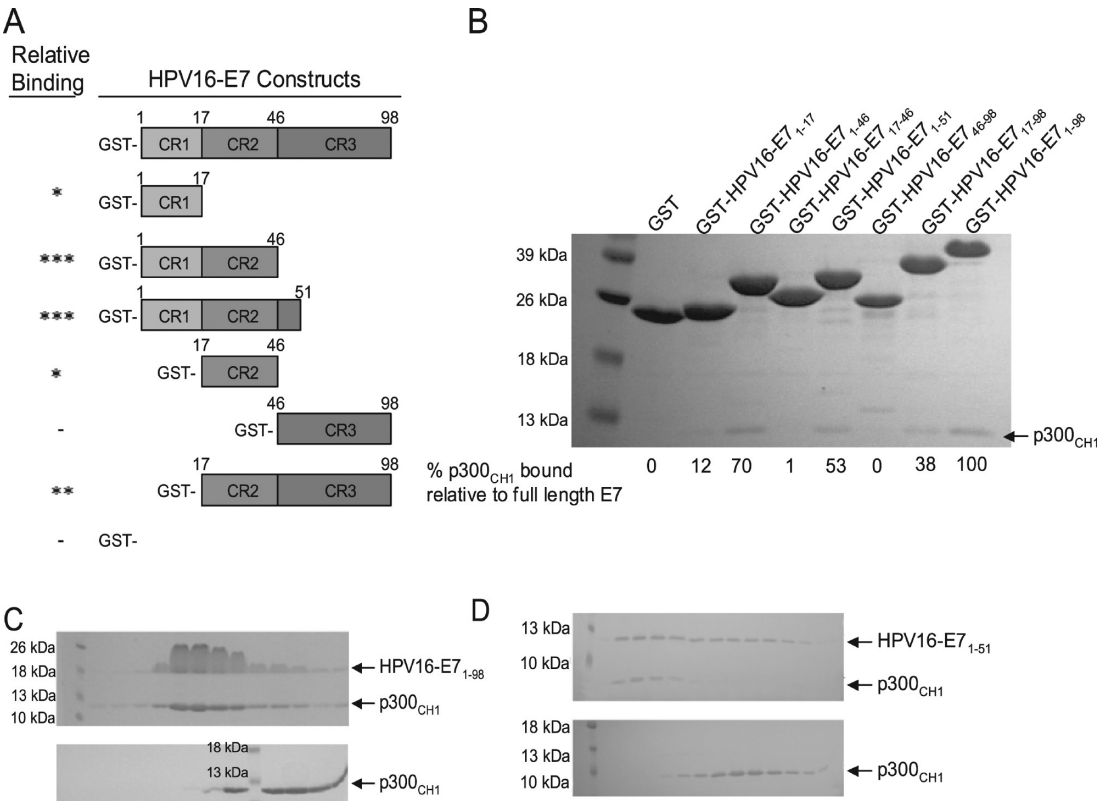

Figure 3. Mapping the interaction between HPV16-E7 and $p300_{CH1}$. (A) Constructs of HPV16-E7 that were tested in pull-down experiments. The asterisks in the left column indicate the level of binding as compared to that of full-length GST-HPV16-$E7_{1-98}$, with more asterisks suggesting a stronger interaction with $p300_{CH1}$. A minus sign indicates that no interaction was observed. (B) Pull downs with the different constructs of HPV16-E7, tagged to GST. An SDS−PAGE gel is shown for each pull down done between $p300_{CH1}$ and the different GST-tagged constructs of HPV16-E7, each tested at a final concentration of 3 μM. GST was used as a control to ensure that $p300_{CH1}$ does not bind to the tag. (C and D) Gel filtration between HPV16-E7 and $p300_{CH1}$. The elution profiles from size exclusion chromatography are shown using SDS−PAGE gels. The elution profile of full-length HPV16-$E7_{1-98}$ (C) in complex with $p300_{CH1}$ (final protein concentrations tested ranging from 40 to 80 μM) is compared to the elution profile of $p300_{CH1}$ alone. Similarly, the elution profile of residues 1−51 of HPV16-E7 (D) in complex with $p300_{CH1}$ (final protein concentrations tested ranging from 40 to 80 μM) is compared to the elution profile of $p300_{CH1}$ alone.

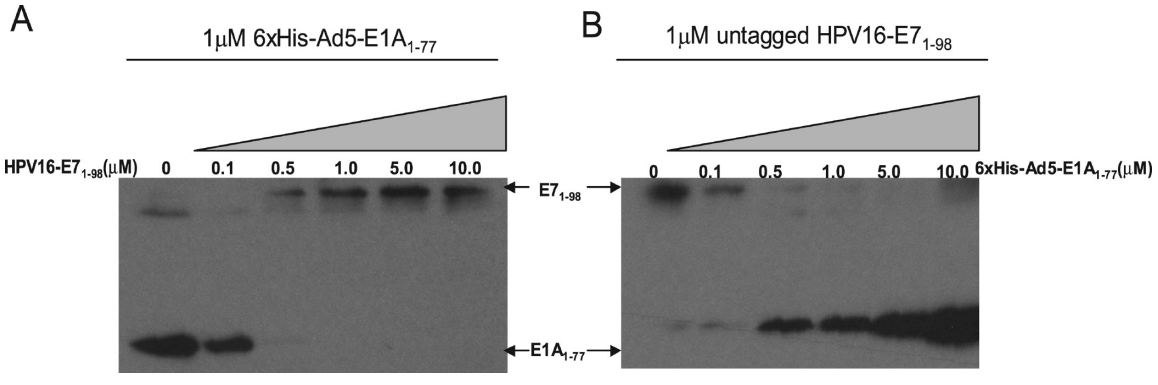

Figure 4. Competition between HPV16-E7 and Ad5-E1A for binding to $p300_{CH1}$. (A) Titration of HPV16-E7 into 6×His-Ad5-$E1A_{1-77}$−$p300_{CH1}$ complexes. Different concentrations of HPV16-$E7_{1-98}$ were added to preformed 6×His-Ad5-$E1A_{1-77}$−$p300_{CH1}$ complexes, and the amount of 6×His-Ad5-$E1A_{1-77}$ remaining bound to GST-$p300_{CH1}$ was probed using an anti-His antibody (left). The amount of HPV16-$E7_{1-98}$ added was probed using anti-HPV16-E7 antibody (left). The higher-molecular mass band in lane 1 corresponds to 6×His-Ad5-$E1A_{1-77}$, because of its high concentration in that sample. (B) Titration of 6×His-Ad5-$E1A_{1-77}$ into HPV16-$E7_{1-98}$−$p300_{CH1}$ complexes. Different concentrations of 6×His-Ad5-$E1A_{1-77}$ were added to preformed HPV16-$E7_{1-98}$−$p300_{CH1}$ complexes, and the amount of HPV16-$E7_{1-98}$ remaining bound to GST-$p300_{CH1}$ was probed using an anti-HPV16-E7 antibody (right). The amount of 6×His-Ad5-$E1A_{1-77}$ added was probed using an anti-His antibody (right). The higher-molecular mass band in lane 6 corresponds to 6×His-Ad5-$E1A_{1-77}$, because of its high concentration in that sample.

do this, analytical ultracentrifugation (AUC) sedimentation equilibrium experiments were performed on the different complexes, as well as on the individual proteins to determine their oligomerization states. In each case, AUC sedimentation equilibrium experiments were performed at 4 °C using protein optical densities of 0.7, 0.5, and 0.3 and three different speeds, and a global fit of the data was performed. A summary of the constructs tested, the protein concentrations used, the speeds

dx.doi.org/10.1021/bi3011863 | *Biochemistry* 2012, 51, 9524−9534

Table 1. Summary of Results from AUC Sedimentation Equilibrium Studies

	concn[a] (μM)	speed[b] (rpm)	model used for fitting	stoichiometry/ oligomerization state	monomer M_w (kDa)	monomer $M_{w(app)}$ (kDa)	K_D[f] (μM)	rmsd[g] (μM)
$p300_{CH1}$	55, 90, 125	24K, 30K, 42.5K	single species	monomer[d]	11.6	12.1[d]	NA[h]	0.017
6×His-Ad5-$E1A_{1-189}$	30, 50, 65	20.5K, 26K, 36K	single species	monomer[d]	24.2	25.9[d]	NA[h]	0.029
6×His-Ad5-$E1A_{1-138}$	65, 110, 160	23K, 28K, 40K	single species	monomer[d]	18.3	19.6[d]	NA[h]	0.029
Ad5-$E1A_{1-77}$	NC[i]	NC[i]	NC[i]	NC[i]	8.5	NC[i]	NA[h]	NC[i]
6×His-Ad5-$E1A_{1-189}$–$p300_{CH1}$	30, 50, 65	16K, 20.5K, 30K	A + B ↔ AB[c]	1:1[e]	NA[h]	NA[h]	0.32	0.026
6×His-Ad5-$E1A_{1-138}$–$p300_{CH1}$	50, 80, 115	19K, 23K, 34K	A + B ↔ AB[c]	1:1[e]	NA[h]	NA[h]	0.10	0.025
Ad5-$E1A_{1-77}$–$p300_{CH1}$	100, 170, 240	20K, 24K, 35.5K	A + B ↔ AB[c]	1:1[e]	NA[h]	NA[h]	0.22	0.030
HPV16-$E7_{1-98}$	50, 85, 120	22K, 25.8K, 36.5K	monomer ↔ n-mer[c] (n = 2)	dimer[d]	11.0	11.4[d]	0.53	0.006
HPV16-$E7_{1-51}$	65, 110, 160	26K, 35K, 46K	single species	monomer[d,k]	5.8	5.8[d]	NA[h]	0.018
HPV16- $E7_{1-98}$–$p300_{CH1}$	50, 85, 120	15.5K, 19K, 25.8K	$nA \leftrightarrow A_n$,[c] $A_n + B \leftrightarrow A_nB$[j] ($n$ = 2)	2:2[e]	NA[h]	NA[h]	3.5	0.019
HPV16- $E7_{1-51}$–$p300_{CH1}$	90, 150, 210	19K, 26K, 35K	A + B ↔ AB[c]	1:1[e]	NA[h]	NA[h]	0.88	0.008

[a]Concentrations were chosen so that three different optical densities would be obtained (0.3, 0.5, and 0.7) for each sample. Consequently, proteins with lower extinction coefficients were used at a higher concentration so that visible curves could be obtained. [b]Speeds were chosen such that the ratio of the squares of the highest to lowest speed was greater than 3 and the ratio of the squares of the middle and lowest speed was greater than 1.4. [c]The model chosen for the complexes was determined by the molecular mass as determined using the single-species model. [d]The oligomerization state of the individual proteins and its apparent monomeric weight-average molecular mass were determined by using a single-species model. [e]The binding stoichiometry of the complexes was determined by using the single-species model followed by the indicated model, where the molecular mass for each monomeric protein was used for A and B. [f]A global K_D was determined by analyzing three different concentrations of the protein complex at the different speeds simultaneously. [g]Root-mean-square deviation of the residuals. [h]NA denotes that the information is not applicable. [i]NC denotes data that were not collected. This was due to the poor behavior of of this construct when alone in solution. [j]A molecular mass corresponding to two molecules of $p300_{CH1}$ was used for B. [k]The K_D for dimerization of E7 is comparable to results published previously.[28]

and models employed, and the results obtained is given in Table 1. The data with residuals are provided in Figure S1 of the Supporting Information for two of the complexes. The residuals were randomly distributed above and below the baseline, indicative of good fits. To ensure that the proteins and their respective complexes stayed in solution, experiments with HPV16-E7 were conducted in a buffer consisting of 20 mM Tris, 50 mM NaCl, and 1 mM TCEP, where the pH was adjusted to 8.0 for full-length HPV16-E7 and to 7.0 for HPV16-$E7_{1-51}$. Experiments with Ad5-E1A were conducted in a buffer consisting of 20 mM Tris (pH 8.0), 100 mM NaCl, and 1 mM TCEP. Complexes were prerun via gel filtration prior to their analysis using analytical ultracentrifugation sedimentation equilibrium experiments.

The individual proteins $p300_{CH1}$, 6×His-Ad5-$E1A_{1-189}$, 6×His-Ad5-$E1A_{1-138}$, and HPV16-$E7_{1-51}$ were fit to a single-species model, and their apparent molecular masses were generally within 10% of their actual molecular masses, suggesting they were monomers when alone in solution (Table 1). Untagged Ad5-$E1A_{1-77}$ precipitated when alone in solution and could therefore not be tested using this technique. HPV16-$E7_{1-98}$, which is known to dimerize, was fit to a monomer ↔ dimer equilibrium, and its monomeric molecular mass was also found to be within 10% of its actual molecular mass. Furthermore, its K_D was found to be 0.53 μM, similar to what was reported previously.[28]

For the complexes between the viral oncoproteins and $p300_{CH1}$, the data were first fit to a single-species model to determine the molecular mass of the complex and the binding stoichiometry. In all cases except for the HPV16-$E7_{1-98}$–$p300_{CH1}$ complex, the molecular mass of the complex corresponded to a 1:1 $p300_{CH1}$–viral oncoprotein complex (Table 1). Therefore, in these cases, the A + B ↔ AB model was used for fitting, where the molecular masses of each protein were used for A and B. In the case of the HPV16-$E7_{1-98}$–$p300_{CH1}$ complex, the molecular mass of the complex appeared to be approximately 40 kDa, so the $2A \leftrightarrow A_2$, $A_2 + B \leftrightarrow A_2B$ model was used for fitting the data, where twice the molecular mass of $p300_{CH1}$ was used for B. The model fit well, indicating that the HPV16-$E7_{1-98}$–$p300_{CH1}$ complex binding stoichiometry is 2:2.

The dissociation constants for binding of $p300_{CH1}$ to 6×His-Ad5-$E1A_{1-189}$, 6×His-Ad5-$E1A_{1-138}$, and 6×His-Ad5-$E1A_{1-77}$ were calculated to be 320, 100, and 220 nM, respectively, suggesting a strong interaction between Ad5-E1A and $p300_{CH1}$. HPV16-E7 was found to bind more weakly to $p300_{CH1}$, consistent with our results using pull downs. The dissociation constants for binding of HPV16-$E7_{1-98}$ and HPV16-$E7_{1-51}$ to $p300_{CH1}$ were found to be 3.5 and 0.88 μM, respectively.

Ad5-E1A, but Not HPV16-E7, Can Form a Ternary Complex with p300 and pRb. Given that the CR2 domain of HPV16-E7 and the CR1 and CR2 domains of Ad5-E1A bind to the pocket domain of pRb,[26,27,32,33] and that we were able to show that these same domains bind to $p300_{CH1}$, we were interested in determining whether $p300_{CH1}$ and the pRb pocket domain bind competitively or form a ternary complex with the viral oncoproteins. For these studies, we employed a pRb pocket domain that is missing the loop between the A and B cyclin folds ($pRb_{AB\Delta loop}$) and therefore forms a globular heterodimer but forms two bands on SDS–PAGE (see lane 3 of Figure 5). We first conducted pull-down studies with GST-Ad5-$E1A_{1-77}$ and GST-Ad5-$E1A_{1-138}$, which were immobilized

dx.doi.org/10.1021/bi3011863 | Biochemistry 2012, 51, 9524–9534

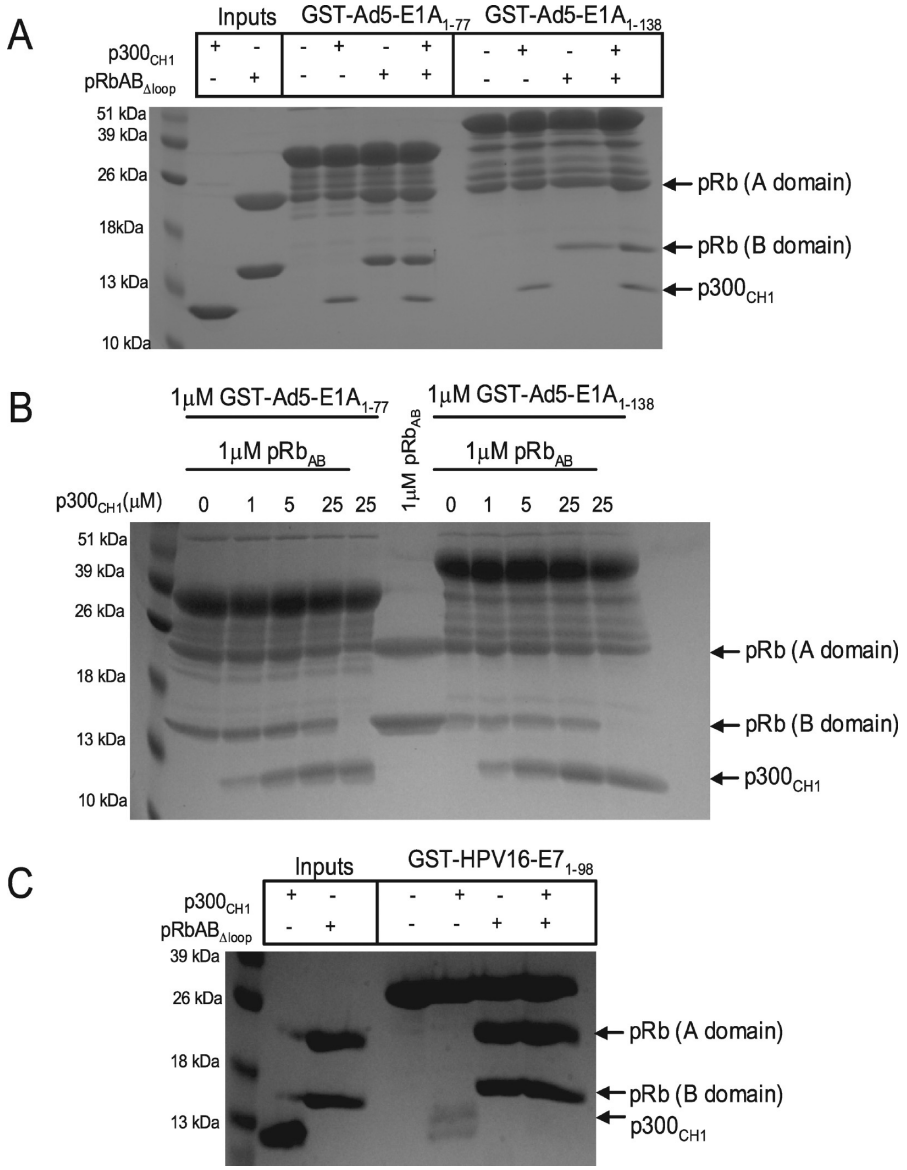

Figure 5. Formation of the ternary complex viral oncoprotein with $p300_{CH1}$ and $pRb_{AB\Delta loop}$. (A) Pull downs between GST-Ad5-$E1A_{1-77}$ or GST-Ad5-$E1A_{1-138}$ and $p300_{CH1}$ and $pRb_{AB\Delta loop}$. An SDS−PAGE gel is shown in which equimolar amounts of $p300_{CH1}$ alone, $pRb_{AB\Delta loop}$ alone, or both $p300_{CH1}$ and $pRb_{AB\Delta loop}$ were added to the indicated construct of GST-Ad5-E1A on GST beads (final concentration of 1 μM). (B) Titration of $p300_{CH1}$ into GST-Ad5-E1A−pRb_{AB}, complexes. Five-fold dilutions of $p300_{CH1}$, starting at 25 μM, were added to the preformed GST-Ad5-E1A−$pRb_{AB\Delta loop}$ or GST-Ad5-E1A−$pRb_{AB\Delta loop}$ complex on GST beads to see if $p300_{CH1}$ could compete $pRb_{AB\Delta loop}$ off. The maximal amount of $p300_{CH1}$ that could bind to GST-Ad5-E1A is shown in the lanes in which $pRb_{AB\Delta loop}$ was not added. (C) Pull downs among GST-HPV16-$E7_{1-98}$, $p300_{CH1}$, and $pRb_{AB\Delta loop}$ (final concentration of 2.6 μM). An SDS−PAGE gel is shown in which equimolar amounts of $p300_{CH1}$ alone, $pRb_{AB\Delta loop}$ alone, or both $p300_{CH1}$ and $pRb_{AB\Delta loop}$ were added to GST-HPV16-$E7_{1-98}$ on GST beads. The amount of proteins remaining bound is shown using an SDS−PAGE gel.

on GST-resin with the addition of $p300_{CH1}$, $pRb_{AB\Delta loop}$, or both proteins. Proteins were tested at a final concentration of 1 μM. The proteins bound to Ad5-E1A were identified by running the samples on SDS−PAGE gels. These experiments revealed that both $p300_{CH1}$ and $pRb_{AB\Delta loop}$ alone and in combination formed a complex with both forms of Ad5-E1A (Figure 5A). To ensure that both $p300_{CH1}$ and $pRb_{AB\Delta loop}$ could bind simultaneously to Ad5-E1A, the experiment in which increasing amounts of $p300_{CH1}$, with respect to a 25-fold excess over pRb and Ad5-E1A, were added to preformed $pRb_{AB\Delta loop}$−GST-Ad5-E1A complexes was repeated. $p300_{CH1}$ did not appear to compete off $pRb_{AB\Delta loop}$ from either GST-Ad5-$E1A_{1-77}$ or GST-Ad5-$E1A_{1-138}$, suggesting that a ternary complex can form among these three proteins (Figure 5B). Interestingly, analogous pull-down studies with GST-HPV16-$E7_{1-98}$ did not reveal the presence of an analogous ternary complex between $p300_{CH1}$ and $pRb_{AB\Delta loop}$ (Figure 5C), suggesting that there are molecular differences for how Ad-E1A and HPV-E7 encage $p300_{CH1}$ for disruption of p300 activity.

■ DISCUSSION

Our gel filtration and analytical ultracentrifugation sedimentation equilibrium data show that the interactions between the viral oncoproteins and $p300_{CH1}$ are significant. The proteins were shown to bind with a 1:1 stochiometry and with dissociation constants for the Ad5-E1A−$p300_{CH1}$ and

dx.doi.org/10.1021/bi3011863 | Biochemistry 2012, 51, 9524−9534

HPV16-E7−$p300_{CH1}$ complexes in the midnanomolar and low micromolar range, respectively. The poorer dissociation constants (0.88−3.5 μM) for the HPV16-E7−$p300_{CH1}$ complex could be due to the fact that either additional regions of p300 are necessary for the interaction or additional proteins may be needed to further stabilize this complex. The K_D values of 100−320 nM that were obtained for the Ad5-E1A−$p300_{CH1}$ complex, on the other hand, suggest that this interaction is very stable. Interestingly, the interaction between low-risk HPV1A-E7, which is generally associated with benign lesions, and $p300_{CH1}$ was much weaker than that between high-risk HPV16-E7, which is known to cause a number of cancers, and $p300_{CH1}$.[34−36] Consistent with our results, others have also shown that there is a stronger interaction between high-risk HPV16-E7 and p300 than between a different low-risk E7 protein, from HPV11, and p300.[18] This suggests that the high-risk HPV16-E7−$p300_{CH1}$ interaction could contribute to cellular transformation and cancer. This is also consistent with results showing that Ad5-E1A can cause cellular transformation by its interaction with p300.[14−17] The ∼10-fold difference in the dissociation constant between HPV16-E7 and Ad5-E1A binding to p300 suggests that they may induce p300-mediated cellular transformation by different mechanisms.

Taking together the fact that the dissociation constants determined by analytical ultracentrifugation sedimentation equilibrium were similar (within 4-fold) for several different truncation constructs of each viral oncoprotein with $p300_{CH1}$, and that these proteins exhibited similar binding to $p300_{CH1}$ using pull downs and gel filtration, we were able to map regions of the viral oncoproteins necessary for the interaction. Whereas the unstructured CR1 and CR2 domains of HPV16-E7 (residues 1−46) were needed for binding to $p300_{CH1}$, the N-terminus and CR1 domains of Ad5-E1A (residues 1−77) were required for binding. It is possible that $p300_{CH1}$ is recruited by the CR1 and CR2 domains of HPV16-E7 and the N-terminus and CR1 domains of Ad5-E1A, after which p300 histone acetyltransferase (HAT) activity is inhibited by the other domains of the viral oncoproteins. This has already been demonstrated for E1A,[37] and because Ad-E1A and HPV-E7 are functionally homologous, HPV-E7 may work the same way.

While others were able to show formation of a ternary complex among the CR1 domain of E1A, the CH3 domain of p300, and pRb,[13] we were also able to show that a ternary complex can form with the CH1 domain of p300, as well. On the other hand, we could not detect a complex of HPV16-E7 with $p300_{CH1}$ and pRb. Formation of a ternary complex among Ad5-E1A, pRb, and p300 could result in a deregulation of pRb acetylation by p300 and therefore a change in pRb phosphorylation by cyclin-dependent kinases.[8] This can then result in an aberration of cell cycle control because pRb is a regulator of the G1 to S phase transition of the cell cycle.[38−40] The fact that we were unable to detect an analogous ternary complex with HPV16-E7 supports the hypothesis that HPV16-E7 may induce cellular transformation by a different mechanism. It is also possible that the interaction between each viral oncoprotein and p300 may result in a modulation of other acetylated targets, such as histones, thereby providing another route through which Ad-E1A and HPV-E7 may influence gene regulation and result in cellular transformation.[7]

Because both Ad5-E1A and HPV16-E7 were shown to bind competitively to $p300_{CH1}$, this suggests that they may bind to the same surface of p300. Interestingly, the CH1 domain of p300 can bind many transcription factors using different parts of its surface. For example, the NMR structures of transcription factor HIF-1α and the CITED2 transactivator were determined in complex with the CH1 (TAZ1) domain of CBP, which is very similar to the corresponding domain of $p300_{CH1}$, and shown to bind the TAZ1 domain in different ways.[22,41] It is also possible that the two viral oncoproteins compete with each other by some allosteric mechanism that involves binding to distinct sites on $p300_{CH1}$. This would be consistent with the divergence of sequence between the regions of Ad-E1A and HPV-E7 that mediate $p300_{CH1}$ interaction. Either way, HPV-E7 and Ad-E1A may interfere with a certain subset of transcription factors to either activate or repress transcription. Therefore, the viral oncoproteins can cause cellular transformation by disrupting important protein complexes in addition to modulating the HAT activity of p300. Notably, p53, which is an important transcription regulator and modulator of protein function, has also been suggested to bind to the CH1 domain of p300.[42,43] Therefore, it is possible that one way in which HPV-E7 and Ad-E1A can lead to cellular transformation is by interfering with the normal activities between p300 and p53. Alternatively, these viral oncoproteins may also interfere with the binding of p300 and MDM2, a negative regulator of p53, also shown to bind to the CH1 domain of p300.[44] Although additional studies are clearly required to delineate the molecular details of regulation of p300 by the HPV-E7 and Ad-E1A viral oncoproteins, our studies represent the first important demonstration that these viral oncoproteins use nonhomologous regions to bind to the same p300 CH1 domain to disrupt p300 function by distinct mechanisms. This may be analogous to how HPV-E7 and Ad-E1A both disrupt pRb function by binding to the same pRb pocket domain but through distinct molecular mechanisms.[26,27,29] Indeed, it appears that DNA tumor viruses have evolved several different strategies for disrupting normal cellular functions.

■ ASSOCIATED CONTENT

Supporting Information

Analytical ultracentrifugation sedimentation equilibrium curves of two different $p300_{CH1}$−viral oncoprotein complexes and their corresponding residual curves. This material is available free of charge via the Internet at http://pubs.acs.org.

■ AUTHOR INFORMATION

Corresponding Author

*E-mail: marmor@wistar.org. Phone: (215) 898-5006.

Funding

This work was supported by National Institutes of Health (NIH) Grants CA094165 and GM060293 and a Hiliary Koprowski, M.D., Professorship awarded to R.M. D.F. was supported by NIH Training Grant GM071339. We acknowledge support of the Protein Expression and Libraries and Proteomics core facilities at the Wistar Institute (supported by NIH Grant CA010815) for the studies presented here.

Notes

The authors declare no competing financial interest.

■ REFERENCES

(1) Janknecht, R. (2002) The versatile functions of the transcriptional coactivators p300 and CBP and their roles in disease. *Histol. Histopathol. 17*, 657−668.

(2) Giordano, A., and Avantaggiati, M. L. (1999) p300 and CBP: Partners for life and death. *J. Cell. Physiol. 181*, 218−230.

(3) Goodman, R. H., and Smolik, S. (2000) CBP/p300 in cell growth, transformation, and development. *Genes Dev. 14*, 1553−1577.
(4) Shikama, N., Lee, C. W., France, S., Delavaine, L., Lyon, J., Krstic-Demonacos, M., and La Thangue, N. B. (1999) A novel cofactor for p300 that regulates the p53 response. *Mol. Cell 4*, 365−376.
(5) Chan, H. M., and La Thangue, N. B. (2001) p300/CBP proteins: HATs for transcriptional bridges and scaffolds. *J. Cell Sci. 114*, 2363−2373.
(6) Blobel, G. A. (2000) CREB-binding protein and p300: Molecular integrators of hematopoietic transcription. *Blood 95*, 745−755.
(7) Ogryzko, V. V., Schiltz, R. L., Russanova, V., Howard, B. H., and Nakatani, Y. (1996) The transcriptional coactivators p300 and CBP are histone acetyltransferases. *Cell 87*, 953−959.
(8) Chan, H. M., Krstic-Demonacos, M., Smith, L., Demonacos, C., and La Thangue, N. B. (2001) Acetylation control of the retinoblastoma tumour-suppressor protein. *Nat. Cell Biol. 3*, 667−674.
(9) Grossman, S. R. (2001) p300/CBP/p53 interaction and regulation of the p53 response. *Eur. J. Biochem. 268*, 2773−2778.
(10) Giles, R. H., Peters, D. J., and Breuning, M. H. (1998) Conjunction dysfunction: CBP/p300 in human disease. *Trends Genet. 14*, 178−183.
(11) Gayther, S. A., Batley, S. J., Linger, L., Bannister, A., Thorpe, K., Chin, S. F., Daigo, Y., Russell, P., Wilson, A., Sowter, H. M., Delhanty, J. D., Ponder, B. A., Kouzarides, T., and Caldas, C. (2000) Mutations truncating the EP300 acetylase in human cancers. *Nat. Genet. 24*, 300−303.
(12) Eckner, R., Ewen, M. E., Newsome, D., Gerdes, M., DeCaprio, J. A., Lawrence, J. B., and Livingston, D. M. (1994) Molecular cloning and functional analysis of the adenovirus E1A-associated 300-kD protein (p300) reveals a protein with properties of a transcriptional adaptor. *Genes Dev. 8*, 869−884.
(13) Ferreon, J. C., Martinez-Yamout, M. A., Dyson, H. J., and Wright, P. E. (2009) Structural basis for subversion of cellular control mechanisms by the adenoviral E1A oncoprotein. *Proc. Natl. Acad. Sci. U.S.A. 106*, 13260−13265.
(14) Ferrari, R., Pellegrini, M., Horwitz, G. A., Xie, W., Berk, A. J., and Kurdistani, S. K. (2008) Epigenetic reprogramming by adenovirus e1a. *Science 321*, 1086−1088.
(15) Turnell, A. S., and Mymryk, J. S. (2006) Roles for the coactivators CBP and p300 and the APC/C E3 ubiquitin ligase in E1A-dependent cell transformation. *Br. J. Cancer 95*, 555−560.
(16) Wang, H. G., Moran, E., and Yaciuk, P. (1995) E1A promotes association between p300 and pRB in multimeric complexes required for normal biological activity. *J. Virol. 69*, 7917−7924.
(17) Ait-Si-Ali, S., Polesskaya, A., Filleur, S., Ferreira, R., Duquet, A., Robin, P., Vervish, A., Trouche, D., Cabon, F., and Harel-Bellan, A. (2000) CBP/p300 histone acetyl-transferase activity is important for the G1/S transition. *Oncogene 19*, 2430−2437.
(18) Bernat, A., Avvakumov, N., Mymryk, J. S., and Banks, L. (2003) Interaction between the HPV E7 oncoprotein and the transcriptional coactivator p300. *Oncogene 22*, 7871−7881.
(19) Zimmermann, H., Degenkolbe, R., Bernard, H. U., and O'Connor, M. J. (1999) The human papillomavirus type 16 E6 oncoprotein can down-regulate p53 activity by targeting the transcriptional coactivator CBP/p300. *J. Virol. 73*, 6209−6219.
(20) Patel, D., Huang, S. M., Baglia, L. A., and McCance, D. J. (1999) The E6 protein of human papillomavirus type 16 binds to and inhibits co-activation by CBP and p300. *EMBO J. 18*, 5061−5072.
(21) De Guzman, R. N., Wojciak, J. M., Martinez-Yamout, M. A., Dyson, H. J., and Wright, P. E. (2005) CBP/p300 TAZ1 domain forms a structured scaffold for ligand binding. *Biochemistry 44*, 490−497.
(22) Freedman, S. J., Sun, Z. Y., Poy, F., Kung, A. L., Livingston, D. M., Wagner, G., and Eck, M. J. (2002) Structural basis for recruitment of CBP/p300 by hypoxia-inducible factor-1α. *Proc. Natl. Acad. Sci. U.S.A. 99*, 5367−5372.
(23) Kurokawa, R., Kalafus, D., Ogliastro, M. H., Kioussi, C., Xu, L., Torchia, J., Rosenfeld, M. G., and Glass, C. K. (1998) Differential use of CREB binding protein-coactivator complexes. *Science 279*, 700−703.
(24) Barbosa, M. S., Edmonds, C., Fisher, C., Schiller, J. T., Lowy, D. R., and Vousden, K. H. (1990) The region of the HPV E7 oncoprotein homologous to adenovirus E1a and Sv40 large T antigen contains separate domains for Rb binding and casein kinase II phosphorylation. *EMBO J. 9*, 153−160.
(25) Dyson, N., Guida, P., Munger, K., and Harlow, E. (1992) Homologous sequences in adenovirus E1A and human papillomavirus E7 proteins mediate interaction with the same set of cellular proteins. *J. Virol. 66*, 6893−6902.
(26) Lee, J. O., Russo, A. A., and Pavletich, N. P. (1998) Structure of the retinoblastoma tumour-suppressor pocket domain bound to a peptide from HPV E7. *Nature 391*, 859−865.
(27) Liu, X., and Marmorstein, R. (2007) Structure of the retinoblastoma protein bound to adenovirus E1A reveals the molecular basis for viral oncoprotein inactivation of a tumor suppressor. *Genes Dev. 21*, 2711−2716.
(28) Clements, A., Johnston, K., Mazzarelli, J. M., Ricciardi, R. P., and Marmorstein, R. (2000) Oligomerization properties of the viral oncoproteins adenovirus E1A and human papillomavirus E7 and their complexes with the retinoblastoma protein. *Biochemistry 39*, 16033−16045.
(29) Liu, X., Clements, A., Zhao, K., and Marmorstein, R. (2006) Structure of the Human Papillomavirus Oncoprotein and Its Mechanism for Inactivation of the Retinoblastoma Tumor Suppressor. *J. Biol. Chem. 281*, 578−586.
(30) Xiao, B., Spencer, J., Clements, A., Ali-Khan, N., Mittnacht, S., Broceno, C., Burghammer, M., Perrakis, A., Marmorstein, R., and Gamblin, S. J. (2003) Crystal structure of the retinoblastoma tumor suppressor protein bound to E2F and the molecular basis of its regulation. *Proc. Natl. Acad. Sci. U.S.A. 100*, 2363−2368.
(31) Laue, T. M., Shah, B. F., Ridgeway, T. M., and Pelletier, S. L. (1992) *Analytical Ultracentrifugation in Biochemistry and Polymer Science*, Royal Society of Chemistry, London.
(32) Fattaey, A. R., Harlow, E., and Helin, K. (1993) Independent regions of adenovirus E1A are required for binding to and dissociation of E2F-protein complexes. *Mol. Cell. Biol. 13*, 7267−7277.
(33) Ikeda, M. A., and Nevins, J. R. (1993) Identification of distinct roles for separate E1A domains in disruption of E2F complexes. *Mol. Cell. Biol. 13*, 7029−7035.
(34) Burd, E. M. (2003) Human papillomavirus and cervical cancer. *Clin. Microbiol. Rev. 16*, 1−17.
(35) zur Hausen, H. (2002) Papillomaviruses and cancer: From basic studies to clinical application. *Nat. Rev. Cancer 2*, 342−350.
(36) zur Hausen, H. (1996) Papillomavirus infections: A major cause of human cancers. *Biochim. Biophys. Acta 1288*, F55−F78.
(37) Chakravarti, D., Ogryzko, V., Kao, H. Y., Nash, A., Chen, H., Nakatani, Y., and Evans, R. M. (1999) A viral mechanism for inhibition of p300 and PCAF acetyltransferase activity. *Cell 96*, 393−403.
(38) Grana, X., Garriga, J., and Mayol, X. (1998) Role of the retinoblastoma protein family, pRB, p107 and p130 in the negative control of cell growth. *Oncogene 17*, 3365−3383.
(39) Harbour, J. W., and Dean, D. C. (2000) The Rb/E2F pathway: Expanding roles and emerging paradigms. *Genes Dev. 14*, 2393−2409.
(40) Harbour, J. W., Luo, R. X., Dei Santi, A., Postigo, A. A., and Dean, D. C. (1999) Cdk phosphorylation triggers sequential intramolecular interactions that progressively block Rb functions as cells move through G1. *Cell 98*, 859−869.
(41) Freedman, S. J., Sun, Z. Y., Kung, A. L., France, D. S., Wagner, G., and Eck, M. J. (2003) Structural basis for negative regulation of hypoxia-inducible factor-1α by CITED2. *Nat. Struct. Biol. 10*, 504−512.
(42) Teufel, D. P., Freund, S. M., Bycroft, M., and Fersht, A. R. (2007) Four domains of p300 each bind tightly to a sequence spanning both transactivation subdomains of p53. *Proc. Natl. Acad. Sci. U.S.A. 104*, 7009−7014.
(43) Kim, H. J., Kim, H. J., Lim, S. C., Kim, S. H., and Kim, T. Y. (2003) Induction of apoptosis and expression of cell cycle regulatory

proteins in response to a phytosphingosine derivative in HaCaT human keratinocyte cells. *Mol. Cells 16*, 331−337.
(44) Kobet, E., Zeng, X., Zhu, Y., Keller, D., and Lu, H. (2000) MDM2 inhibits p300-mediated p53 acetylation and activation by forming a ternary complex with the two proteins. *Proc. Natl. Acad. Sci. U.S.A. 97*, 12547−12552.